Investigation of the effect of compressibility on acoustic radiation in Low-Mach-Number flows using different LES model

Asiye Karakus*†, Stephen Turnock†,Phillip Joseph*,and Chaitanya Paruchuri* †Maritime Engineering, University of Southampton, * ISVR, University of Southampton a.karakus@soton.ac.uk

Introdiction

Noise generated by the flow around bluff or streamlined bodies is still a significant engineering challenge. This unintended noise issue arises in numerous applications, including air conditioners, refrigerator cooling fans, helicopter-drone propellers, ship propellers, aircraft wings and rotors, landing gears, and wind turbines. Additionally, the rising concern over ocean noise pollution has emphasized the need to address this problem to protect passengers, crew, and marine life, with particular significance from a military viewpoint. Analysing hydrodynamic noise caused by turbulent flow over lifting surfaces can be tackled through theoretical approaches and numerical methods, such as computational fluid dynamics. However, comprehending the chaotic interaction between upstream turbulence and sound propagation remains a complex task, requiring innovative solutions. Managing noise generated by flow around different bodies is a multifaceted challenge with wide-ranging implications across various industries. As advances are made in understanding noise generation and propagation, the pursuit of effective noise reduction methods becomes increasingly critical.

Literature Review

At high Reynolds numbers, flow around a bluff body - such as a circular cylinder - will become turbulent and separate. This creates instabilities in the wake region, known in the literature as the von Karman Vortex Street. The drag and lift fluctuations on the bluff body caused by vortex shedding from a stationary cylinder in the flow are the main sources of noise. The noise is characterized by dipole and quadrupole patterns, resulting from the drag and lift fluctuations on the body and the unsteady wake behind the bluff body, respectively (You et al., 1998). To mitigate this noise, it is recommended to use a plate as a flow controller to disrupt the von Karman Vortex Street and reduce the lift and drag fluctuations and vortex shedding noise. Lighthill, 1952, proposed the noise mechanism generated by a turbulent flow. In this theory Lighthill produced acoustic analogy just for a free field. After this first approach, Curle, 1955, developed a general formulation for bluff body surface in fluid. Following these, Ffowcs Williams and Hawkings, 1969, generalized the formulation further for moving boundaries. Amiet, 1973 predicted the broadband noise spectrum for single airfoils in turbulent flows by combining Sear's theory with acoustic analogies. Although analytical models, that require simplifying assumptions about the turbulent flow and the airfoil geometry, are cheap and fast for simple geometries, numerical approaches in the time domain offer a promising alternative for complex geometries. As a result, new CFD approaches that are commonly used for aeroacoustic predictions in complex flows must be examined in light of current computer resources as a road map for future applications in an industrial context. Such as large-eddy simulation (LES), which predicts larger turbulent structures of the flow down to the spatial filter size, assuming that their sound radiation dominates the lower end of the acoustic spectrum(Boudet et al., 2005). As a benchmark study for broadband noise, Jacob et al., 2005 examined a rod-airfoil configuration in wind tunnel with low Mach number. The flow around the rod attached to the basement and NACA-0012 has been studied, taken into account the effects of three dimensions. In the measurements made, there is a 2 mm deviation between the rod and the centre of the airfoil due to the airfoil geometry. They used two different diameters (0.01, 0.016 meter) and four different velocities for each diameter (30.5, 65, 72, 115 m/s) to understand the behaviour of flow. Strong 3-D effects, secondary vortex, vortex splitting, and stretching significantly deflect the flowfield. Due to these effects spectral broadening around the shedding frequency and its harmonics happened. As a summary, the most dominant source region is the foil leading edge where the secondary vortex is created. Later, Boudet et al., 2005

conducted a numerical study with using LES turbulence model. They managed to catch high agreement with the experimental results with the LES method. In their numerical study, Han et al., 2023 showed the effect of span-wise length on noise prediction with using LES. In this present study, based on the high success of numerical methods such as LES in broadband noise prediction, we will try to examine the effect of compressibility on acoustic noise radiation using the same method.

Methodology

The interaction of the turbulent velocity field with leading edge of a flat plate cause the acoustic surface pressure and radiation. The Amiet model gives an comprehensive explanation for a single turbulent gust encountered with the flat plate (Amiet, 1973). In the analytic model we assume that a vertical single turbulent gust has a uniform convection velocity in positive x-direction. The gust vertical velocity can be written with the help of gust wave-number component. The pressure distribution (ΔP) for an incompressible gust on the airfoil can be shown as:

$$P(x,t) = \rho_0 U w_0 \sqrt{\frac{1-x}{1+x}} S(k) e^{i\omega t}$$
(1)

where w_0 is vertical velocity of a single gust and S(k) is Sears function depends on the k which is acoustic reduced frequency. Sears function can be represented in the following way;

$$S(k) = \frac{2}{\pi k} \frac{1}{H_0^{(2)}(k) - iH_1^{(2)}(k)}$$
 (2)

where $H_0^{(2)}(k)$ and $H_1^{(2)}(k)$ are Hankel functions.

Similarly the pressure distributions (ΔP) for a compressible gust on the airfoil can be shown as : For small kM:

$$P_{Am}(x,t) = \mp \rho_0 \frac{U}{\beta} w_0 S(k') \sqrt{\frac{1-x}{1+x}} e^{i(\omega t + k'M^2 x)} e^{ikf(M)/\beta^2}$$
(3)

where $k' = \frac{k}{\beta^2}$ and source term is $f(M) = (1 - \beta) \ln M + \beta \ln(1 + \beta) - \ln 2$. For large kM:

$$P(x,t) = P_1(x,t) + P_2(x,t)$$
(4)

$$P_1(x,t) = \mp \frac{\rho_0 U w_0}{\sqrt{(1+M)\pi kx}} e^{i(\omega t + \frac{Mkx}{1+M} - \pi/4)}$$
 (5)

$$P_2(x,t) = \mp \frac{\rho_0 U w_0}{\sqrt{2\pi (1+M)k}} \left[\sqrt{2} E^* \left(\sqrt{\frac{2kM}{\beta^2} (2-x)} e^{i\pi/4} - 1 \right] e^{i(\omega t - \frac{kMx}{1+M} - \pi/4)} \right]$$
 (6)

where E^* is a complex conjugate of Fresnal integral.

As can be understood from the equation, we will be able to observe the effect of the Mach number. Far field approximation of Green's function can be shown as:

$$\frac{\partial G}{\partial y}(x, y, X, w) \approx \frac{iy}{4} \sqrt{\frac{2k_0}{\pi \sigma^3}} e^{-i\frac{k_0}{\beta^2} [\sigma - Xx/\sigma - M(x-X)] + i\frac{3\pi}{4}}$$
(7)

where $\sigma = \sqrt{x^2 + \beta^2 y^2}$ and x and y represent the observer location $x = rsin(\theta)$ and $y = rcos(\theta)$.

The same Green's function have been used to radiate the pressure distributions along the chord which obtained numerically.

For the numerical analysis the pressure values at the flat plate surface are calculated by solving the continuity and momentum equations in a compressible form. The continuity equation is given as:

$$\frac{\partial \rho_0}{\partial t} + \nabla \cdot (\rho_0 U) = 0 \tag{8}$$

here ρ represent the fluid density and ${\bf U}$ mean velocity of fluid.

The momentum equation is given as:

$$\frac{\partial(\rho U)}{\partial t} + \nabla \cdot ((\rho U) \otimes U) = -\nabla P + 2\mu(S - \frac{1}{3}(\nabla U)I) \tag{9}$$

here p is the fluid pressure, μ is the dynamic viscosity of the fluid, **I** is the identity matrix and **S** the symmetric part of strain rate tensor.

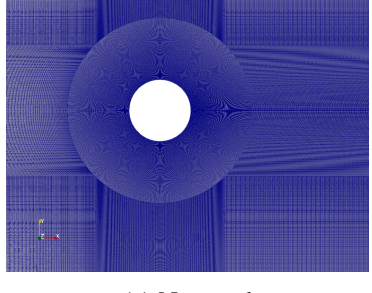
$$S = \frac{1}{2} (\nabla U + (\nabla U)^T) \tag{10}$$



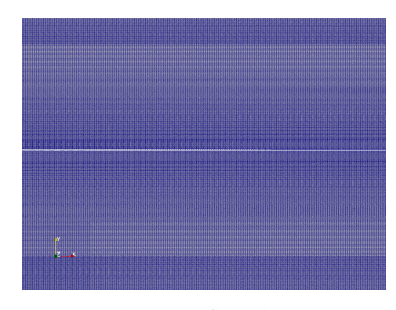
Fig. 1: Computational domain

The problem at hand involves the flow of a single-phase fluid around a circular rod with a free-stream velocity U. To disrupt the flow and reduce noise, a thin flat plate is placed downstream of the rod, with both the rod and plate sharing the same centre axis. The thickness of the plate is D/10, and the chord length is 10D. The distance between the rod and plate is one chord length. The upstream length of the domain is 15D,

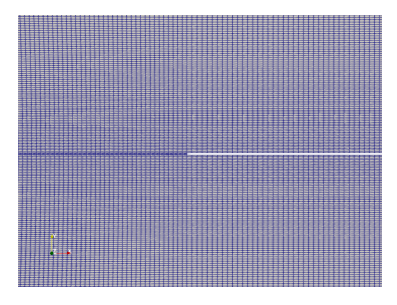
and the downstream flow field extends to 41D. The boundaries on the vertical axis extend to 15D on both sides. A velocity inlet is chosen for the left-hand side of Figure 1, while a pressure outlet is chosen for the right-hand side. Slip boundary conditions are chosen for pressure on the surface of the cylinder and plate to calculate their response. The remaining surfaces, including the top, bottom, and faces, are chosen as symmetrical. In Figure 2 structured mesh are presented near the boundaries. All simulations have been conducted by using OpenFOAM. As an compressible adiabatic solver rhoPimpleAdiabaticFoam is used. First RANS equations are solved until the flow reached steady state regime, then RANS solution is used as an input for LES simulation. Table 1 shows simulation settings for each Mach Number.



(a) Near rod



(b) Near flat plate



(c) Leading edge

Fig. 2: Mesh structure

Parameters/ Mach Number	M=0.05	M=0.1	M=0.2
Mesh Type	hexahedra	hexahedra	hexahedra
Mesh size	$1.8 * 10^6$	$1.8 * 10^6$	$1.8 * 10^6$
Δt	$5*10^{-8}$	$5*10^{-10}$	$5*10^{-12}$
Reynolds Number	120000	240000	480000

Table 1: Simulation settings

Results

Velocity spectra at near rod wake can be seen at Figure 3. For each cases the shedding frequency is around 0.2. From the graph, highest peak for rod only case can reach around 20 dB. When the downstream plate is added, the highest peak drops of more than 10 dB. The shedding frequency still can be seen clearly in Figure 4a around 0.2. Similarly, pressure distribution at leading edge for different Mach numbers is shown in Figure 4b. Pressure spectra at downstream along the plate and trailing edge can be seen in Figure 5a and 5b, respectively. As the Mach number decreases, the location of the highest peak shifts forward in both figure 5a and 5b.

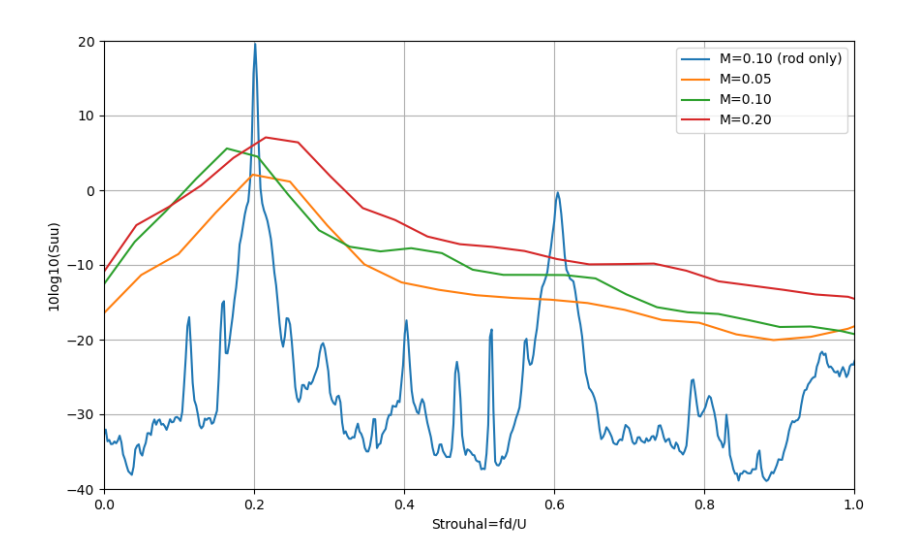


Fig. 3: Velocity spectra near rod wake, x/c=-0.9

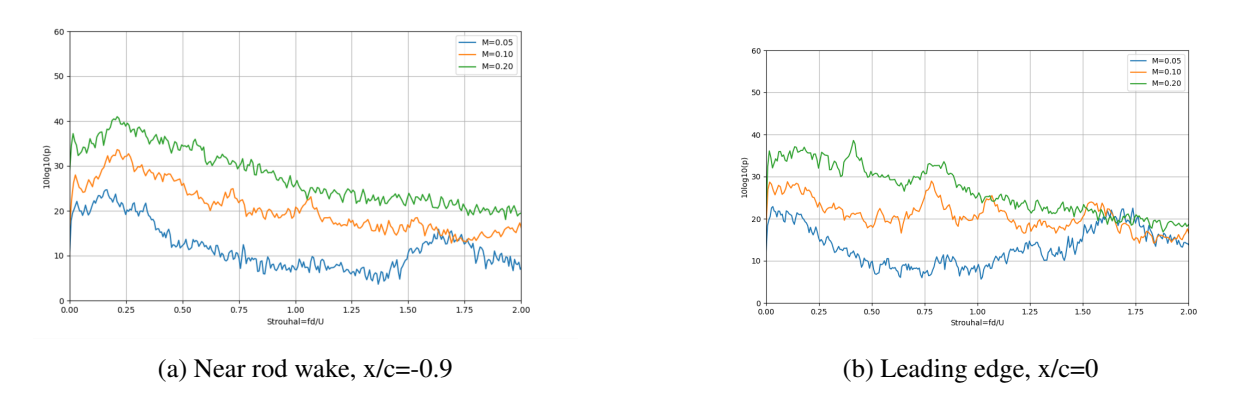
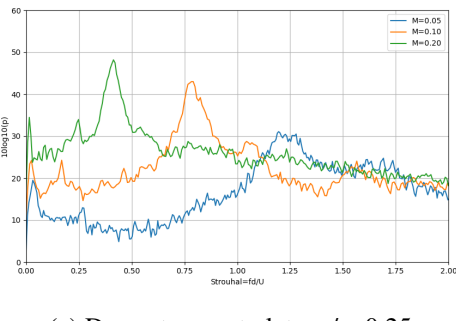
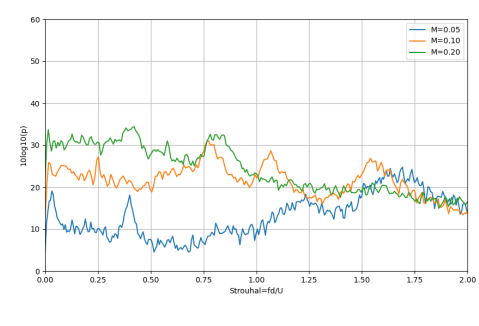


Fig. 4: Pressure Spectra





(a) Downstream at plate, x/c=0.25

(b) Trailing edge, x/c=1

Fig. 5: Pressure Spectra

Conclusions and Future Works

The solutions have been derived at various Mach numbers, with a focus on identifying the critical Mach number where compressibility loses significance. Beyond this critical Mach number, incompressible flow solvers can be employed to continue the solutions, as compressibility effects become negligible. This study aims to determine pressure fluctuations on the plate surface and the consequent acoustic radiation in the far field. This study still is work in progress and the comparison with experimental data and analytic solution will be made.

Acknowledgements

The authors would like to thank the Ministry of Education in Turkey who has supported Asiye Karakus for her Ph.D. studies.

References

Amiet, R. K. (1973). Review of unsteady airfoil lift theories. Technical Report M210885-2, United Aircraft Research Laboratories.

Boudet, J., Grosjean, N., and Jacob, M. C. (2005). Wake-airfoil interaction as broadband noise source: a large-eddy simulation study. *International Journal of Aeroacoustics*, 4(1-2):93–115.

Curle, N. (1955). The influence of solid boundaries upon aerodynamic sound. *Proceedings of the Royal Society of London. Series A. Mathematical and Physical Sciences*, 231(1187):505–514.

Ffowcs Williams, J. E. and Hawkings, D. L. (1969). Sound generation by turbulence and surfaces in arbitrary motion. *Philosophical Transactions of the Royal Society of London. Series A, Mathematical and Physical Sciences*, 264(1151):321–342.

Han, J., Zhang, Y., Li, S., Hong, W., and Wu, D. (2023). The noise-generating mechanism of rod-airfoil configuration and the effect of spanwise length on noise prediction. *Aerospace Science and Technology*, 134:108166.

Jacob, M. C., Boudet, J., Casalino, D., and Michard, M. (2005). A rod-airfoil experiment as a benchmark for broadband noise modeling. *Theoretical and Computational Fluid Dynamics*, 19(3):171–196.

Lighthill, M. J. (1952). On sound generated aerodynamically i. general theory. *Proceedings of the Royal Society of London. Series A. Mathematical and Physical Sciences*, 211(1107):564–587.

You, D., Choi, H., Choi, M.-R., and Kang, S.-H. (1998). Control of flow-induced noise behind a circular cylinder using splitter plates. *AIAA journal*, 36(11):1961–1967.